

Observation of $\chi_{cJ} \rightarrow 3K_S^0 K^\pm \pi^\mp$

- M. Ablikim¹, M. N. Achasov^{4,c}, P. Adlarson⁷⁶, X. C. Ai⁸¹, R. Aliberti³⁵, A. Amoroso^{75A,75C}, Q. An^{72,58,a}, Y. Bai⁵⁷, O. Bakina³⁶, Y. Ban^{46,h}, H.-R. Bao⁶⁴, V. Batozskaya^{1,44}, K. Begzsuren³², N. Berger³⁵, M. Berlowski⁴⁴, M. Bertani^{28A}, D. Bettomini^{29A}, F. Bianchi^{75A,75C}, E. Bianco^{75A,75C}, A. Bortone^{75A,75C}, I. Boyko³⁶, R. A. Briere⁵, A. Brueggemann⁶⁹, H. Cai⁷⁷, M. H. Cai^{38,k,l}, X. Cai^{1,58}, A. Calcaterra^{28A}, G. F. Cao^{1,64}, N. Cao^{1,64}, S. A. Cetin^{62A}, X. Y. Chai^{46,h}, J. F. Chang^{1,58}, G. R. Che⁴³, Y. Z. Che^{1,58,64}, G. Chelkov^{36,b}, C. Chen⁴³, C. H. Chen⁹, Chao Chen⁵⁵, G. Chen¹, H. S. Chen^{1,64}, H. Y. Chen²⁰, M. L. Chen^{1,58,64}, S. J. Chen⁴², S. L. Chen⁴⁵, S. M. Chen⁶¹, T. Chen^{1,64}, X. R. Chen^{31,64}, X. T. Chen^{1,64}, Y. B. Chen^{1,58}, Y. Q. Chen³⁴, Z. J. Chen^{25,i}, Z. K. Chen⁵⁹, S. K. Choi¹⁰, X. Chu^{12,g}, G. Cibinetto^{29A}, F. Cossio^{75C}, J. J. Cui⁵⁰, H. L. Dai^{1,58}, J. P. Dai⁷⁹, A. Dbeyssei¹⁸, R. E. de Boer³, D. Dedovich³⁶, C. Q. Deng⁷³, Z. Y. Deng¹, A. Denig³⁵, I. Denisenko³⁶, M. Destefanis^{75A,75C}, F. De Mori^{75A,75C}, B. Ding^{67,1}, X. X. Ding^{46,h}, Y. Ding⁴⁰, Y. Ding³⁴, Y. X. Ding³⁰, J. Dong^{1,58}, L. Y. Dong^{1,64}, M. Y. Dong^{1,58,64}, X. Dong⁷⁷, M. C. Du¹, S. X. Du⁸¹, Y. Y. Duan⁵⁵, Z. H. Duan⁴², P. Egorov^{36,b}, G. F. Fan⁴², J. J. Fan¹⁹, Y. H. Fan⁴⁵, J. Fang⁵⁹, J. Fang^{1,58}, S. S. Fang^{1,64}, W. X. Fang¹, Y. Q. Fang^{1,58}, R. Farinelli^{29A}, L. Fava^{75B,75C}, F. Feldbauer³, G. Felici^{28A}, C. Q. Feng^{72,58}, J. H. Feng⁵⁹, Y. T. Feng^{72,58}, M. Fritsch³, C. D. Fu¹, J. L. Fu⁶⁴, Y. W. Fu^{1,64}, H. Gao⁶⁴, X. B. Gao⁴¹, Y. N. Gao^{46,h}, Y. N. Gao¹⁹, Y. Y. Gao³⁰, Yang Gao^{72,58}, S. Garbolino^{75C}, I. Garzia^{29A,29B}, P. T. Ge¹⁹, Z. W. Ge⁴², C. Geng⁵⁹, E. M. Gersabeck⁶⁸, A. Gilman⁷⁰, K. Goetzen¹³, J. D. Gong³⁴, L. Gong⁴⁰, W. X. Gong^{1,58}, W. Gradl³⁵, S. Gramigna^{29A,29B}, M. Greco^{75A,75C}, M. H. Gu^{1,58}, Y. T. Gu¹⁵, C. Y. Guan^{1,64}, A. Q. Guo³¹, L. B. Guo⁴¹, M. J. Guo⁵⁰, R. P. Guo⁴⁹, Y. P. Guo^{12,g}, A. Guskov^{36,b}, J. Gutierrez²⁷, K. L. Han⁶⁴, T. T. Han¹, F. Hanisch³, K. D. Hao^{72,58}, X. Q. Hao¹⁹, F. A. Harris⁶⁶, K. K. He⁵⁵, K. L. He^{1,64}, F. H. Heinsius³, C. H. Heinz³⁵, Y. K. Heng^{1,58,64}, C. Herold⁶⁰, T. Holtmann³, P. C. Hong³⁴, G. Y. Hou^{1,64}, X. T. Hou^{1,64}, Y. R. Hou⁶⁴, Z. L. Hou¹, B. Y. Hu⁵⁹, H. M. Hu^{1,64}, J. F. Hu^{56,j}, Q. P. Hu^{72,58}, S. L. Hu^{12,g}, T. Hu^{1,58,64}, Y. Hu¹, Z. M. Hu⁵⁹, G. S. Huang^{72,58}, K. X. Huang⁵⁹, L. Q. Huang^{31,64}, P. Huang⁴², X. T. Huang⁵⁰, Y. P. Huang¹, Y. S. Huang⁵⁹, T. Hussain⁷⁴, N. Hüskens³⁵, N. in der Wiesche⁶⁹, J. Jackson²⁷, S. Janchiv³², Q. Ji¹, Q. P. Ji¹⁹, W. Ji^{1,64}, X. B. Ji^{1,58}, Y. Y. Ji⁵⁰, Z. K. Jia^{72,58}, D. Jiang^{1,64}, H. B. Jiang⁷⁷, P. C. Jiang^{46,h}, S. J. Jiang⁹, T. J. Jiang¹⁶, X. S. Jiang^{1,58,64}, Y. Jiang⁶⁴, J. B. Jiao⁵⁰, J. K. Jiao³⁴, Z. Jiao²³, S. Jin⁴², Y. Jin⁶⁷, M. Q. Jing^{1,64}, X. M. Jing⁶⁴, T. Johansson⁷⁶, S. Kabana³³, N. Kalantar-Nayestanaki⁶⁵, X. L. Kang⁹, X. S. Kang⁴⁰, M. Kavatsyuk⁶⁵, B. C. Ke⁸¹, V. Khachatryan²⁷, A. Khoukaz⁶⁹, R. Kiuchi¹, O. B. Kolcu^{62A}, B. Kopf³, M. Kuessner³, X. Kui^{1,64}, N. Kumar²⁶, A. Kupsc^{44,76}, W. Kühn³⁷, Q. Lan⁷³, W. N. Lan¹⁹, T. T. Lei^{72,58}, Z. H. Lei^{72,58}, M. Lellmann³⁵, T. Lenz³⁵, C. Li⁴³, C. Li⁴⁷, C. H. Li³⁹, C. K. Li²⁰, Cheng Li^{72,58}, D. M. Li⁸¹, F. Li^{1,58}, G. Li¹, H. B. Li^{1,64}, H. J. Li¹⁹, H. N. Li^{56,j}, Hui Li⁴³, J. R. Li⁶¹, J. S. Li⁵⁹, K. Li¹, K. L. Li^{38,k,l}, K. L. Li¹⁹, L. J. Li^{1,64}, Lei Li⁴⁸, M. H. Li⁴³, M. R. Li^{1,64}, P. L. Li⁶⁴, P. R. Li^{38,k,l}, Q. M. Li^{1,64}, Q. X. Li⁵⁰, R. Li^{17,31}, T. Li⁵⁰, T. Y. Li⁴³, W. D. Li^{1,64}, W. G. Li^{1,a}, X. Li^{1,64}, X. H. Li^{72,58}, X. L. Li⁵⁰, X. Y. Li^{1,8}, X. Z. Li⁵⁹, Y. Li¹⁹, Y. G. Li^{46,h}, Y. P. Li³⁴, Z. J. Li⁵⁹, Z. Y. Li⁷⁹, C. Liang⁴², H. Liang^{72,58}, Y. F. Liang⁵⁴, Y. T. Liang^{31,64}, G. R. Liao¹⁴, L. B. Liao⁵⁹, M. H. Liao⁵⁹, Y. P. Liao^{1,64}, J. Libby²⁶, A. Limphirat⁶⁰, C. C. Lin⁵⁵, C. X. Lin⁶⁴, D. X. Lin^{31,64}, L. Q. Lin³⁹, T. Lin¹, B. J. Liu¹, B. X. Liu⁷⁷, C. Liu³⁴, C. X. Liu¹, F. Liu¹, F. H. Liu⁵³, Feng Liu⁶, G. M. Liu^{56,j}, H. Liu^{38,k,l}, H. B. Liu¹⁵, H. H. Liu¹, H. M. Liu^{1,64}, Huihui Liu²¹, J. B. Liu^{72,58}, J. J. Liu²⁰, K. Liu^{38,k,l}, K. Liu⁷³, K. Y. Liu⁴⁰, Ke Liu²², L. Liu^{72,58}, L. C. Liu⁴³, Lu Liu⁴³, P. L. Liu¹, Q. Liu⁶⁴, S. B. Liu⁶⁴, T. Liu^{12,g}, W. K. Liu⁴³, W. M. Liu^{72,58}, W. T. Liu³⁹, X. Liu^{38,k,l}, X. Liu³⁹, X. Y. Liu⁷⁷, Y. Liu⁸¹, Y. Liu^{38,k,l}, Y. Liu⁸¹, Y. B. Liu⁴³, Z. A. Liu^{1,58,64}, Z. D. Liu⁹, Z. Q. Liu⁵⁰, X. C. Lou^{1,58,64}, F. X. Lu⁵⁹, H. J. Lu²³, J. G. Lu^{1,58}, Y. Lu⁷, Y. H. Lu^{1,64}, Y. P. Lu^{1,58}, Z. H. Lu^{1,64}, C. L. Luo⁴¹, J. R. Luo⁵⁹, J. S. Luo^{1,64}, M. X. Luo⁸⁰, T. Luo^{12,g}, X. L. Luo^{1,58}, Z. Y. Lv²², X. R. Lyu^{64,p}, Y. F. Lyu⁴³, Y. H. Lyu⁸¹, F. C. Ma⁴⁰, H. Ma⁷⁹, H. L. Ma¹, J. L. Ma^{1,64}, L. L. Ma⁵⁰, L. R. Ma⁶⁷, Q. M. Ma¹, R. Q. Ma^{1,64}, R. Y. Ma¹⁹, T. Ma^{72,58}, X. T. Ma^{1,64}, X. Y. Ma^{1,58}, Y. M. Ma³¹, F. E. Maas¹⁸, I. MacKay⁷⁰, M. Maggiore^{75A,75C}, S. Malde⁷⁰, Y. J. Mao^{46,h}, Z. P. Mao¹, S. Marcello^{75A,75C}, Y. H. Meng⁶⁴, Z. X. Meng⁶⁷, J. G. Messchendorp^{13,65}, G. Mezzadri^{29A}, H. Miao^{1,64}, T. J. Min⁴², R. E. Mitchell²⁷, X. H. Mo^{1,58,64}, B. Moses²⁷, N. Yu. Muchnoi^{4,c}, J. Muskalla³⁵, Y. Nefedov³⁶, F. Nerling^{18,e}, L. S. Nie²⁰, I. B. Nikolaev^{4,c}, Z. Ning^{1,58}, S. Nisar^{11,m}, Q. L. Niu^{38,k,l}, W. D. Niu^{12,g}, S. L. Olsen^{10,64}, Q. Ouyang^{1,58,64}, S. Pacetti^{28B,28C}, X. Pan⁵⁵, Y. Pan⁵⁷, A. Pathak¹⁰, Y. P. Pei^{72,58}, M. Pelizaeus³, H. P. Peng^{72,58}, Y. Y. Peng^{38,k,l}, K. Peters^{13,e}, J. L. Ping⁴¹, R. G. Ping^{1,64}, S. Plura³⁵, V. Prasad³³, F. Z. Qi¹, H. R. Qi⁶¹, M. Qi⁴², S. Qian^{1,58}, W. B. Qian⁶⁴, C. F. Qiao⁶⁴, J. H. Qiao¹⁹, J. J. Qin⁷³, J. L. Qin⁵⁵, L. Q. Qin¹⁴, L. Y. Qin^{72,58}, P. B. Qin⁷³, X. P. Qin^{12,g}, X. S. Qin⁵⁰, Z. H. Qin^{1,58}, J. F. Qiu¹, Z. H. Qu⁷³, C. F. Redmer³⁵, A. Rivetti^{75C}, M. Rolo^{75C}, G. Rong^{1,64}, S. S. Rong^{1,64}, Ch. Rosner¹⁸, M. Q. Ruan^{1,58}, S. N. Ruan⁴³, N. Salone⁴⁴, A. Sarantsev^{36,d}, Y. Schelhaas³⁵, K. Schoenning⁷⁶, M. Scodeggio^{29A}, K. Y. Shan^{12,g}, W. Shan²⁴, X. Y. Shan^{72,58}, Z. J. Shang^{38,k,l}, J. F. Shangguan¹⁶, L. G. Shao^{1,64}, M. Shao^{72,58}, C. P. Shen^{12,g}, H. F. Shen^{1,8}, W. H. Shen⁶⁴, X. Y. Shen^{1,64},

B. A. Shi⁶⁴, H. Shi^{72,58}, J. L. Shi^{12,g}, J. Y. Shi¹, S. Y. Shi⁷³, X. Shi^{1,58}, H. L. Song^{72,58}, J. J. Song¹⁹, T. Z. Song⁵⁹, W. M. Song^{34,1}, Y. X. Song^{46,h,n}, S. Sosio^{75A,75C}, S. Spataro^{75A,75C}, F. Stieler³⁵, S. S Su⁴⁰, Y. J. Su⁶⁴, G. B. Sun⁷⁷, G. X. Sun¹, H. Sun⁶⁴, H. K. Sun¹, J. F. Sun¹⁹, K. Sun⁶¹, L. Sun⁷⁷, S. S. Sun^{1,64}, T. Sun^{51,f}, Y. C. Sun⁷⁷, Y. H. Sun³⁰, Y. J. Sun^{72,58}, Y. Z. Sun¹, Z. Q. Sun^{1,64}, Z. T. Sun⁵⁰, C. J. Tang⁵⁴, G. Y. Tang¹, J. Tang⁵⁹, L. F. Tang³⁹, M. Tang^{72,58}, Y. A. Tang⁷⁷, L. Y. Tao⁷³, M. Tat⁷⁰, J. X. Teng^{72,58}, V. Thoren⁷⁶, J. Y. Tian^{72,58}, W. H. Tian⁵⁹, Y. Tian³¹, Z. F. Tian⁷⁷, I. Uman^{62B}, B. Wang⁵⁹, B. Wang¹, Bo Wang^{72,58}, C. Wang¹⁹, Cong Wang²², D. Y. Wang^{46,h}, H. J. Wang^{38,k,l}, J. J. Wang⁷⁷, K. Wang^{1,58}, L. L. Wang¹, L. W. Wang³⁴, M. Wang^{72,58}, M. Wang⁵⁰, N. Y. Wang⁶⁴, S. Wang^{38,k,l}, S. Wang^{12,g}, T. Wang^{12,g}, T. J. Wang⁴³, W. Wang⁵⁹, W. Wang⁷³, W. P. Wang^{35,58,72,o}, X. Wang^{46,h}, X. F. Wang^{38,k,l}, X. J. Wang³⁹, X. L. Wang^{12,g}, X. N. Wang¹, Y. Wang⁶¹, Y. D. Wang⁴⁵, Y. F. Wang^{1,58,64}, Y. H. Wang^{38,k,l}, Y. L. Wang¹⁹, Y. N. Wang⁷⁷, Y. Q. Wang¹, Yaqian Wang¹⁷, Yi Wang⁶¹, Yuan Wang^{17,31}, Z. Wang^{1,58}, Z. L. Wang⁷³, Z. Q. Wang^{12,g}, Z. Y. Wang^{1,64}, D. H. Wei¹⁴, H. R. Wei⁴³, F. Weidner⁶⁹, S. P. Wen¹, Y. R. Wen³⁹, U. Wiedner³, G. Wilkinson⁷⁰, M. Wolke⁷⁶, C. Wu³⁹, J. F. Wu^{1,8}, L. H. Wu¹, L. J. Wu^{1,64}, Lianjie Wu¹⁹, S. G. Wu^{1,64}, S. M. Wu⁶⁴, X. Wu^{12,g}, X. H. Wu³⁴, Y. J. Wu³¹, Z. Wu^{1,58}, L. Xia^{72,58}, X. M. Xian³⁹, B. H. Xiang^{1,64}, T. Xiang^{46,h}, D. Xiao^{38,k,l}, G. Y. Xiao⁴², H. Xiao⁷³, Y. L. Xiao^{12,g}, Z. J. Xiao⁴¹, C. Xie⁴², K. J. Xie^{1,64}, X. H. Xie^{46,h}, Y. Xie⁵⁰, Y. G. Xie^{1,58}, Y. H. Xie⁶, Z. P. Xie^{72,58}, T. Y. Xing^{1,64}, C. F. Xu^{1,64}, C. J. Xu⁵⁹, G. F. Xu¹, M. Xu^{72,58}, Q. J. Xu¹⁶, Q. N. Xu³⁰, W. L. Xu⁶⁷, X. P. Xu⁵⁵, Y. Xu⁴⁰, Y. Xu^{12,g}, Y. C. Xu⁷⁸, Z. S. Xu⁶⁴, H. Y. Yan³⁹, L. Yan^{12,g}, W. B. Yan^{72,58}, W. C. Yan⁸¹, W. P. Yan¹⁹, X. Q. Yan^{1,64}, H. J. Yang^{51,f}, H. L. Yang³⁴, H. X. Yang¹, J. H. Yang⁴², R. J. Yang¹⁹, T. Yang¹, Y. Yang^{12,g}, Y. F. Yang⁴³, Y. H. Yang⁴², Y. Q. Yang⁹, Y. X. Yang^{1,64}, Y. Z. Yang¹⁹, M. Ye^{1,58}, M. H. Ye⁸, Junhao Yin⁴³, Z. Y. You⁵⁹, B. X. Yu^{1,58,64}, C. X. Yu⁴³, G. Yu¹³, J. S. Yu^{25,i}, M. C. Yu⁴⁰, T. Yu⁷³, X. D. Yu^{46,h}, Y. C. Yu⁸¹, C. Z. Yuan^{1,64}, H. Yuan^{1,64}, J. Yuan⁴⁵, J. Yuan³⁴, L. Yuan², S. C. Yuan^{1,64}, Y. Yuan^{1,64}, Z. Y. Yuan⁵⁹, C. X. Yue³⁹, Ying Yue¹⁹, A. A. Zafar⁷⁴, S. H. Zeng^{63A,63B,63C,63D}, X. Zeng^{12,g}, Y. Zeng^{25,i}, Y. J. Zeng^{1,64}, Y. J. Zeng⁵⁰, X. Y. Zhai³⁴, Y. H. Zhan⁵⁹, A. Q. Zhang^{1,64}, B. L. Zhang^{1,64}, B. X. Zhang¹, D. H. Zhang⁴³, G. Y. Zhang^{1,64}, G. Y. Zhang¹⁹, H. Zhang^{72,58}, H. Zhang⁸¹, H. C. Zhang^{1,58,64}, H. H. Zhang⁵⁹, H. Q. Zhang^{1,58,64}, H. R. Zhang^{72,58}, H. Y. Zhang^{1,58}, J. Zhang⁸¹, J. Zhang⁵⁹, J. J. Zhang⁵², J. L. Zhang²⁰, J. Q. Zhang⁴¹, J. S. Zhang^{12,g}, J. W. Zhang^{1,58,64}, J. X. Zhang^{38,k,l}, J. Y. Zhang¹, J. Z. Zhang^{1,64}, Jianyu Zhang⁶⁴, L. M. Zhang⁶¹, Lei Zhang⁴², N. Zhang⁸¹, P. Zhang^{1,64}, Q. Zhang¹⁹, Q. Y. Zhang³⁴, R. Y. Zhang^{38,k,l}, S. H. Zhang^{1,64}, Shulei Zhang^{25,i}, X. M. Zhang¹, X. Y. Zhang⁴⁰, X. Y. Zhang⁵⁰, Y. Zhang⁷³, Y. Zhang¹, Y. T. Zhang⁸¹, Y. H. Zhang^{1,58}, Y. M. Zhang³⁹, Z. D. Zhang¹, Z. H. Zhang¹, Z. L. Zhang⁵⁵, Z. L. Zhang³⁴, Z. X. Zhang¹⁹, Z. Y. Zhang⁴³, Z. Y. Zhang⁷⁷, Z. Z. Zhang⁴⁵, Zh. Zh. Zhang¹⁹, G. Zhao¹, J. Y. Zhao^{1,64}, J. Z. Zhao^{1,58}, L. Zhao¹, Lei Zhao^{72,58}, M. G. Zhao⁴³, N. Zhao⁷⁹, R. P. Zhao⁶⁴, S. J. Zhao⁸¹, Y. B. Zhao^{1,58}, Y. L. Zhao⁵⁵, Y. X. Zhao^{31,64}, Z. G. Zhao^{72,58}, A. Zhemchugov^{36,b}, B. Zheng⁷³, B. M. Zheng³⁴, J. P. Zheng^{1,58}, W. J. Zheng^{1,64}, X. R. Zheng¹⁹, Y. H. Zheng^{64,p}, B. Zhong⁴¹, X. Zhong⁵⁹, H. Zhou^{35,50,o}, J. Q. Zhou³⁴, J. Y. Zhou³⁴, S. Zhou⁶, X. Zhou⁷⁷, X. K. Zhou⁶, X. R. Zhou^{72,58}, X. Y. Zhou³⁹, Y. Z. Zhou^{12,g}, Z. C. Zhou²⁰, A. N. Zhu⁶⁴, J. Zhu⁴³, K. Zhu¹, K. J. Zhu^{1,58,64}, K. S. Zhu^{12,g}, L. Zhu³⁴, L. X. Zhu⁶⁴, S. H. Zhu⁷¹, T. J. Zhu^{12,g}, W. D. Zhu^{12,g}, W. D. Zhu⁴¹, W. J. Zhu¹, W. Z. Zhu¹⁹, Y. C. Zhu^{72,58}, Z. A. Zhu^{1,64}, X. Y. Zhuang⁴³, J. H. Zou¹, J. Zu^{72,58}

(BESIII Collaboration)

¹ Institute of High Energy Physics, Beijing 100049, People's Republic of China

² Beihang University, Beijing 100191, People's Republic of China

³ Bochum Ruhr-University, D-44780 Bochum, Germany

⁴ Budker Institute of Nuclear Physics SB RAS (BINP), Novosibirsk 630090, Russia

⁵ Carnegie Mellon University, Pittsburgh, Pennsylvania 15213, USA

⁶ Central China Normal University, Wuhan 430079, People's Republic of China

⁷ Central South University, Changsha 410083, People's Republic of China

⁸ China Center of Advanced Science and Technology, Beijing 100190, People's Republic of China

⁹ China University of Geosciences, Wuhan 430074, People's Republic of China

¹⁰ Chung-Ang University, Seoul, 06974, Republic of Korea

¹¹ COMSATS University Islamabad, Lahore Campus, Defence Road, Off Raiwind Road, 54000 Lahore, Pakistan

¹² Fudan University, Shanghai 200433, People's Republic of China

¹³ GSI Helmholtzcentre for Heavy Ion Research GmbH, D-64291 Darmstadt, Germany

¹⁴ Guangxi Normal University, Guilin 541004, People's Republic of China

¹⁵ Guangxi University, Nanning 530004, People's Republic of China

¹⁶ Hangzhou Normal University, Hangzhou 310036, People's Republic of China

- ¹⁷ Hebei University, Baoding 071002, People's Republic of China
¹⁸ Helmholtz Institute Mainz, Staudinger Weg 18, D-55099 Mainz, Germany
¹⁹ Henan Normal University, Xinxiang 453007, People's Republic of China
²⁰ Henan University, Kaifeng 475004, People's Republic of China
²¹ Henan University of Science and Technology, Luoyang 471003, People's Republic of China
²² Henan University of Technology, Zhengzhou 450001, People's Republic of China
²³ Huangshan College, Huangshan 245000, People's Republic of China
²⁴ Hunan Normal University, Changsha 410081, People's Republic of China
²⁵ Hunan University, Changsha 410082, People's Republic of China
²⁶ Indian Institute of Technology Madras, Chennai 600036, India
²⁷ Indiana University, Bloomington, Indiana 47405, USA
²⁸ INFN Laboratori Nazionali di Frascati , (A)INFN Laboratori Nazionali di Frascati, I-00044, Frascati, Italy; (B)INFN Sezione di Perugia, I-06100, Perugia, Italy; (C)University of Perugia, I-06100, Perugia, Italy
²⁹ INFN Sezione di Ferrara, (A)INFN Sezione di Ferrara, I-44122, Ferrara, Italy; (B)University of Ferrara, I-44122, Ferrara, Italy
³⁰ Inner Mongolia University, Hohhot 010021, People's Republic of China
³¹ Institute of Modern Physics, Lanzhou 730000, People's Republic of China
³² Institute of Physics and Technology, Peace Avenue 54B, Ulaanbaatar 13330, Mongolia
³³ Instituto de Alta Investigación, Universidad de Tarapacá, Casilla 7D, Arica 1000000, Chile
³⁴ Jilin University, Changchun 130012, People's Republic of China
³⁵ Johannes Gutenberg University of Mainz, Johann-Joachim-Becher-Weg 45, D-55099 Mainz, Germany
³⁶ Joint Institute for Nuclear Research, 141980 Dubna, Moscow region, Russia
³⁷ Justus-Liebig-Universitaet Giessen, II. Physikalisches Institut, Heinrich-Buff-Ring 16, D-35392 Giessen, Germany
³⁸ Lanzhou University, Lanzhou 730000, People's Republic of China
³⁹ Liaoning Normal University, Dalian 116029, People's Republic of China
⁴⁰ Liaoning University, Shenyang 110036, People's Republic of China
⁴¹ Nanjing Normal University, Nanjing 210023, People's Republic of China
⁴² Nanjing University, Nanjing 210093, People's Republic of China
⁴³ Nankai University, Tianjin 300071, People's Republic of China
⁴⁴ National Centre for Nuclear Research, Warsaw 02-093, Poland
⁴⁵ North China Electric Power University, Beijing 102206, People's Republic of China
⁴⁶ Peking University, Beijing 100871, People's Republic of China
⁴⁷ Qufu Normal University, Qufu 273165, People's Republic of China
⁴⁸ Renmin University of China, Beijing 100872, People's Republic of China
⁴⁹ Shandong Normal University, Jinan 250014, People's Republic of China
⁵⁰ Shandong University, Jinan 250100, People's Republic of China
⁵¹ Shanghai Jiao Tong University, Shanghai 200240, People's Republic of China
⁵² Shanxi Normal University, Linfen 041004, People's Republic of China
⁵³ Shanxi University, Taiyuan 030006, People's Republic of China
⁵⁴ Sichuan University, Chengdu 610064, People's Republic of China
⁵⁵ Soochow University, Suzhou 215006, People's Republic of China
⁵⁶ South China Normal University, Guangzhou 510006, People's Republic of China
⁵⁷ Southeast University, Nanjing 211100, People's Republic of China
⁵⁸ State Key Laboratory of Particle Detection and Electronics, Beijing 100049, Hefei 230026, People's Republic of China
⁵⁹ Sun Yat-Sen University, Guangzhou 510275, People's Republic of China
⁶⁰ Suranaree University of Technology, University Avenue 111, Nakhon Ratchasima 30000, Thailand
⁶¹ Tsinghua University, Beijing 100084, People's Republic of China
⁶² Turkish Accelerator Center Particle Factory Group, (A)Istinye University, 34010, Istanbul, Turkey; (B)Near East University, Nicosia, North Cyprus, 99138, Mersin 10, Turkey
⁶³ University of Bristol, H H Wills Physics Laboratory, Tyndall Avenue, Bristol, BS8 1TL, UK
⁶⁴ University of Chinese Academy of Sciences, Beijing 100049, People's Republic of China
⁶⁵ University of Groningen, NL-9747 AA Groningen, The Netherlands

- ⁶⁶ University of Hawaii, Honolulu, Hawaii 96822, USA
⁶⁷ University of Jinan, Jinan 250022, People's Republic of China
⁶⁸ University of Manchester, Oxford Road, Manchester, M13 9PL, United Kingdom
⁶⁹ University of Muenster, Wilhelm-Klemm-Strasse 9, 48149 Muenster, Germany
⁷⁰ University of Oxford, Keble Road, Oxford OX13RH, United Kingdom
⁷¹ University of Science and Technology Liaoning, Anshan 114051, People's Republic of China
⁷² University of Science and Technology of China, Hefei 230026, People's Republic of China
⁷³ University of South China, Hengyang 421001, People's Republic of China
⁷⁴ University of the Punjab, Lahore-54590, Pakistan
⁷⁵ University of Turin and INFN, (A)University of Turin, I-10125, Turin, Italy; (B)University of Eastern Piedmont, I-15121, Alessandria, Italy; (C)INFN, I-10125, Turin, Italy
⁷⁶ Uppsala University, Box 516, SE-75120 Uppsala, Sweden
⁷⁷ Wuhan University, Wuhan 430072, People's Republic of China
⁷⁸ Yantai University, Yantai 264005, People's Republic of China
⁷⁹ Yunnan University, Kunming 650500, People's Republic of China
⁸⁰ Zhejiang University, Hangzhou 310027, People's Republic of China
⁸¹ Zhengzhou University, Zhengzhou 450001, People's Republic of China

^a Deceased

^b Also at the Moscow Institute of Physics and Technology, Moscow 141700, Russia

^c Also at the Novosibirsk State University, Novosibirsk, 630090, Russia

^d Also at the NRC "Kurchatov Institute", PNPI, 188300, Gatchina, Russia

^e Also at Goethe University Frankfurt, 60323 Frankfurt am Main, Germany

^f Also at Key Laboratory for Particle Physics, Astrophysics and Cosmology, Ministry of Education; Shanghai Key Laboratory for Particle Physics and Cosmology; Institute of Nuclear and Particle Physics, Shanghai 200240, People's Republic of China

^g Also at Key Laboratory of Nuclear Physics and Ion-beam Application (MOE) and Institute of Modern Physics, Fudan University, Shanghai 200443, People's Republic of China

^h Also at State Key Laboratory of Nuclear Physics and Technology, Peking University, Beijing 100871, People's Republic of China

ⁱ Also at School of Physics and Electronics, Hunan University, Changsha 410082, China

^j Also at Guangdong Provincial Key Laboratory of Nuclear Science, Institute of Quantum Matter, South China Normal University, Guangzhou 510006, China

^k Also at MOE Frontiers Science Center for Rare Isotopes, Lanzhou University, Lanzhou 730000, People's Republic of China

^l Also at Lanzhou Center for Theoretical Physics, Lanzhou University, Lanzhou 730000, People's Republic of China

^m Also at the Department of Mathematical Sciences, IBA, Karachi 75270, Pakistan

ⁿ Also at Ecole Polytechnique Federale de Lausanne (EPFL), CH-1015 Lausanne, Switzerland

^o Also at Helmholtz Institute Mainz, Staudinger Weg 18, D-55099 Mainz, Germany

^p Also at Hangzhou Institute for Advanced Study, University of Chinese Academy of Sciences, Hangzhou 310024, China

By analyzing $(2712.4 \pm 14.3) \times 10^6$ $\psi(3686)$ events collected with the BESIII detector operating at the BEPCII collider, the decays $\chi_{c0,1,2} \rightarrow 3K_S^0 K^\pm \pi^\mp$ are observed for the first time with statistical significances greater than 10σ . The branching fractions of these decays are determined to be $\mathcal{B}(\chi_{c0} \rightarrow 3K_S^0 K^\pm \pi^\mp) = (7.95 \pm 0.50 \pm 0.65) \times 10^{-5}$, $\mathcal{B}(\chi_{c1} \rightarrow 3K_S^0 K^\pm \pi^\mp) = (2.62 \pm 0.08 \pm 0.19) \times 10^{-4}$, and $\mathcal{B}(\chi_{c2} \rightarrow 3K_S^0 K^\pm \pi^\mp) = (1.72 \pm 0.07 \pm 0.15) \times 10^{-4}$, where the first uncertainties are statistical and the second systematic.

I. INTRODUCTION

The experimental studies of hadronic decays of the charmonium states are crucial for understanding Quantum Chromodynamics (QCD) models and QCD-based calculations [1–3], since charmonium physics lies in

the transition region between perturbative and non-perturbative QCD. At present, both experimental and theoretical studies of hadronic decays of $\chi_{cJ}(J=0,1,2)$ states are not as extensive as for the vector charmonium states J/ψ and $\psi(3686)$ (almost 30% of the χ_{cJ} decays are not observed based on the total width), and

more measurements are needed. Since the χ_{cJ} mesons are produced copiously in the $\psi(3686)$ radiative decays, with branching fractions of about 9%, the world's largest $\psi(3686)$ data sample at BESIII [8] offers good opportunities to study their different decays. Currently, there have been theoretical predictions and experimental measurements of multi-body-meson decays of χ_{cJ} [4–6]; however, the information of five-body hadronic χ_{cJ} decays is still very limited, and additional experimental measurements of these decays are needed.

In 2015, BESIII reported the measurement of the branching fractions of $\chi_{cJ} \rightarrow \bar{K}^0 K^\pm \pi^\mp \phi$ and $\chi_{cJ} \rightarrow K^+ K^- \pi^0 \phi$ decays in the final state $\chi_{cJ} \rightarrow K K K K \pi$ [4, 7], by using 106×10^6 $\psi(3686)$ events. The obtained results are listed in Table I. In the limit of isospin symmetry, the branching fractions of the $\chi_{cJ} \rightarrow 3K_S^0 K^\pm \pi^\mp$ decays are expected to be at 10^{-4} level, which are accessible at BESIII but have not been studied to date. In this paper, we determine the branching fractions of $\chi_{cJ} \rightarrow 3K_S^0 K^\pm \pi^\mp$ for the first time by analyzing $(2712.4 \pm 14.3) \times 10^6$ $\psi(3686)$ events collected with the BESIII detector.

TABLE I. The world average values ($\times 10^{-4}$) of the branching fractions of the decays contributing to $\chi_{cJ} \rightarrow K K K K \pi$.

	χ_{c0}	χ_{c1}	χ_{c2}
$\bar{K}^0 K^\pm \pi^\mp \phi$	37 ± 6	33 ± 5	48 ± 7
$K^+ K^- \pi^0 \phi$	19.0 ± 3.5	16.2 ± 3.0	27 ± 5

II. BESIII DETECTOR AND MONTE CARLO SIMULATION

The BESIII detector [9] records symmetric e^+e^- collisions provided by the BEPCII storage ring [10] in the center-of-mass energy range from 1.84 to 4.95 GeV, with a peak luminosity of $1.1 \times 10^{33} \text{ cm}^{-2}\text{s}^{-1}$ achieved at $\sqrt{s} = 3.773 \text{ GeV}$.

The cylindrical core of the BESIII detector covers 93% of the full solid angle and consists of a helium-based multilayer drift chamber (MDC), a plastic scintillator time-of-flight system (TOF), and a CsI(Tl) electromagnetic calorimeter (EMC), which are all enclosed in a superconducting solenoidal magnet providing a 1.0 T magnetic field. The magnetic field was 0.9 T in 2012, which affects 12.7% of the total $\psi(3686)$ data. The solenoid is supported by an octagonal flux-return yoke with resistive plate counter muon identification modules interleaved with steel. The charged-particle momentum resolution at 1 GeV/c is 0.5%, and the dE/dx resolution is 6% for electrons from Bhabha scattering. The EMC measures photon energies with a resolution of 2.5% (5%) at 1 GeV in the barrel (end-cap) region. The time resolution in the TOF barrel region is 68 ps, while that in the end cap region was 110 ps. The end-cap TOF system was upgraded in 2015 using multi-gap resistive plate chamber technology, providing a time resolution of 60 ps [11–13],

which benefits 83.3% of the data used in this analysis.

Simulated data samples produced with a GEANT4-based [14] Monte Carlo (MC) package, which includes the geometric description of the BESIII detector and the detector response, are used to determine detection efficiencies and to estimate backgrounds. The simulation includes the beam energy spread and initial state radiation (ISR) in the e^+e^- annihilations with the generator KKMC [15].

The inclusive MC sample includes the production of the $\psi(3686)$ resonance, the ISR production of the J/ψ , and the continuum processes incorporated in KKMC [15]. All particle decays are modelled with EVTGEN [16, 17] using branching fractions either taken from the Particle Data Group (PDG) [4], when available, or otherwise estimated with LUNDCHARM [18]. Final state radiation (FSR) from charged final state particles is incorporated using the PHOTOS package [19]. An inclusive MC sample containing 2.747×10^9 generic $\psi(3686)$ events is used to study background. To account for effects of intermediate resonance structures on the efficiency, each of the $\chi_{c0,1,2}$ is modeled using 200,000 mixed MC events, in which the dominant decay modes containing resonances are included. Particle decays are generated by EVTGEN [16, 17] for the known decay modes with branching fractions taken from the PDG [4]. The other decays are generated by the phase-space (PHSP) model. The mixing ratios of resonances are determined by examining the corresponding invariant mass distributions as discussed in Section IV, which are shown in Table II.

III. EVENT SELECTION

Candidate events are reconstructed via the charmonium transitions $\psi(3686) \rightarrow \gamma \chi_{cJ}$ followed by the hadronic decays $\chi_{cJ} \rightarrow 3K_S^0 K^\pm \pi^\mp$. They are required to contain at least eight charged tracks and at least one photon candidate.

Charged tracks (not originating from K_S^0 decays) are required to be within a polar angle (θ) range of $|\cos\theta| < 0.93$, where θ is defined with respect to the z axis, which is the symmetry axis of the MDC. The distance of closest approach to the interaction point (IP) must be less than 10 cm along the z axis, $|V_z|$, and less than 1 cm in the transverse plane, $|V_{xy}|$.

Photon candidates are identified using showers in the EMC. The deposited energy of each shower must be more than 25 MeV in the barrel region ($|\cos\theta| < 0.80$) and more than 50 MeV in the end-cap region ($0.86 < |\cos\theta| < 0.92$). To exclude showers originating from charged tracks, the angle subtended by the EMC shower and the position of the closest charged track at the EMC must be greater than 10° as measured from the IP. To suppress electronic noise and showers unrelated to the event, the difference between the EMC time and the event start time is required to be within $[0, 700]$ ns.

Particle identification (PID) for charged tracks com-

bines measurements of the specific energy loss (dE/dx) in the MDC and the flight time in the TOF to form likelihoods $\mathcal{L}(h)$ ($h = K, \pi$) for each hadron hypothesis h . Charged kaons and pions are identified by comparing the likelihoods for the kaon and pion hypotheses and requiring $\mathcal{L}(K) > \mathcal{L}(\pi)$ and $\mathcal{L}(\pi) > \mathcal{L}(K)$, respectively.

Each K_S^0 candidate is reconstructed from two oppositely charged tracks satisfying $|V_z| < 20$ cm. The two charged tracks are assigned as $\pi^+\pi^-$ without imposing further PID criteria. They are constrained to originate from a common vertex. The decay length of the K_S^0 candidate is required to be greater than twice the vertex resolution away from the IP. The quality of the vertex fits is required to be $\chi^2 < 200$. The K_S^0 signal region is set to be within 3σ , $|M_{\pi^+\pi^-} - 0.498| < 0.012$ GeV/ c^2 , and the sideband regions are set to be within 5σ and 11σ , $0.020 < |M_{\pi^+\pi^-} - 0.498| < 0.044$ GeV/ c^2 . Figure 1 shows the $M_{\pi^+\pi^-}$ distribution of the accepted candidates in data.

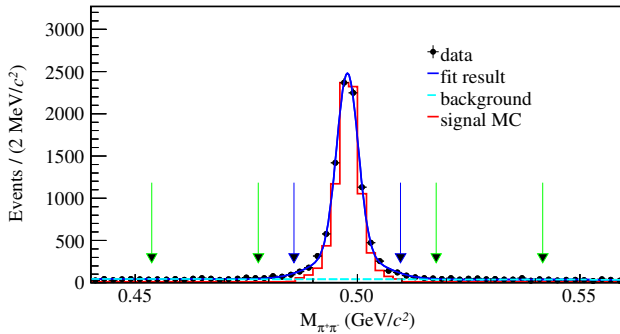


FIG. 1. The $M_{\pi^+\pi^-}$ distribution of the accepted candidates. Dots with error bars represent the data, the blue line is the fit result, the red line is the signal MC sample and the green line the background. The signal MC sample is normalized to have the maximum height of the data. The pair of blue arrows shows the K_S^0 signal region, and the pairs of green arrows show the K_S^0 sideband regions.

A four-constraint (4C) kinematic fit is performed under the hypothesis $\psi(3686) \rightarrow \gamma 3K_S^0 K^\pm \pi^\mp$, by requiring the total reconstructed four-momentum to be conserved. In each event, if more than one combination survives, the one with the smallest χ^2_{4C} from the 4C kinematic fit is retained. The requirement on χ^2_{4C} is optimized with the Figure-of-Merit (FOM) defined as

$$\text{FOM} = \frac{S}{\sqrt{S + B}}, \quad (1)$$

where S is the number of events from the signal MC sample, normalized according to the pre-measured branching fractions without the FOM optimization, and B is the number of background events from the inclusive MC sample, normalized to the data size. From the optimization, we choose $\chi^2_{4C} < 50$ as the nominal requirement.

The potential background components from $\psi(3686)$ decays are studied by analyzing the inclusive MC sample

with a generic event type analysis tool, TopoAna [20]. The peaking background in inclusive MC can be described by the K_S^0 sideband events in data, while the remaining background in inclusive MC is flat. Furthermore, we examine the data sample taken at $\sqrt{s} = 3.650$ GeV, corresponding to an integrated luminosity of 0.4 fb^{-1} [21]. The background at this energy point is found to be negligible.

IV. BRANCHING FRACTION

To determine the signal yields, a simultaneous unbinned maximum likelihood fit is performed on the $M_{3K_S^0 K^\pm \pi^\mp}$ distributions of the accepted candidate events in the K_S^0 signal and sideband regions. In this analysis, the combinatorial background in the $M_{\pi^+\pi^-}$ -distribution is assumed to be flat. Thus, the net numbers of the $\chi_{cJ} \rightarrow 3K_S^0 K^\pm \pi^\mp$ decays can be calculated by

$$N_{\text{net}} = N_{\text{sig}} - \frac{1}{2}N_{\text{SB1}} + \frac{1}{4}N_{\text{SB2}} - \frac{1}{8}N_{\text{SB3}}, \quad (2)$$

where N_{sig} is the number of events with three $\pi^+\pi^-$ pairs lying in the K_S^0 signal region, called the Signal region; N_{SB1} is the number of events with two $\pi^+\pi^-$ pairs lying in the K_S^0 signal region and the other one lying in the K_S^0 sideband region, called the SB1 region; N_{SB2} is the number of events with one $\pi^+\pi^-$ pair lying in the K_S^0 signal region and the other two lying in the K_S^0 sideband region, called the SB2 region; N_{SB3} is the number of events with three $\pi^+\pi^-$ pairs lying in the K_S^0 sideband region, called the SB3 region. Figure 2 shows the three-dimensional distribution of the invariant mass of the three $\pi^+\pi^-$ pairs in data.

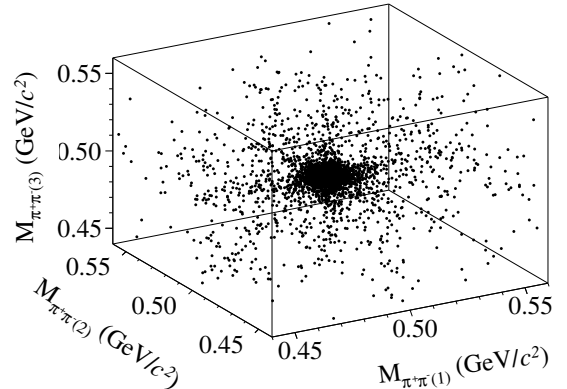


FIG. 2. Distribution of $M_{\pi^+\pi^-_{(1)}} : M_{\pi^+\pi^-_{(2)}} : M_{\pi^+\pi^-_{(3)}}$ for the candidate events in data.

In the fit, the signal shape of the χ_{cJ} states is modeled by using a Breit-Wigner function convolved with a Gaussian function with free parameters, to take into account the resolution. The mass and width of each Breit-

Wigner function are fixed to the respective values from the PDG. The backgrounds are described by a first-order Chebychev polynomial function for the events from both the K_S^0 signal and sideband regions. Figure 3 shows the fit results. Significant χ_{cJ} signals are seen for the events in the signal region, while there are also some peaking background events from the sideband regions. The number of peaking background events in the signal region is estimated to be $\frac{1}{2}N_{\text{SB1}} - \frac{1}{4}N_{\text{SB2}} + \frac{1}{8}N_{\text{SB3}}$, as defined before. From this fit, the signal yields of χ_{c0} , χ_{c1} and χ_{c2} decays, $N_{\chi_{cJ}}^{\text{obs}}$, are obtained to be 343 ± 22 , 1190 ± 36 and 767 ± 29 , respectively. The statistical significances are larger than 10σ for all χ_{cJ} decays, which are estimated by comparing the likelihood values of the fit with and without each signal component and taking into account the number of degrees of freedom.

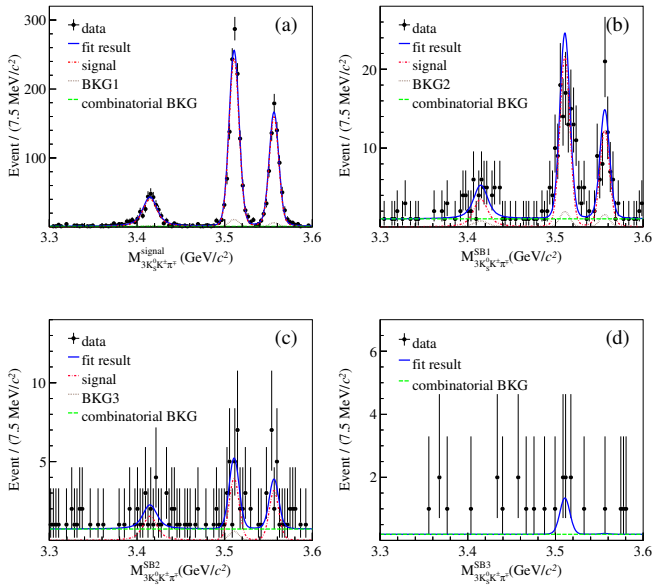


FIG. 3. Simultaneous fit to the $M_{3K_S^0 K^\pm \pi^\mp}$ distributions of the accepted candidate events for $\chi_{cJ} \rightarrow 3K_S^0 K^\pm \pi^\mp$ in data (dots with error bars) in the (a) Signal, (b) SB1, (c) SB2, and (d) SB3 regions, where BKG1, BKG2 and BKG3 stay for the fixed peaking background events from the fitted signal event candidates of sideband regions (b)(c) and (d). The blue solid curves are the fit results, the red curves are the signal shapes, the brown curves are the backgrounds constrained by the K_S^0 sidebands, and the green curves are the fitted backgrounds.

The detection efficiencies of $\psi(3686) \rightarrow \gamma\chi_{cJ}$ with $\chi_{cJ} \rightarrow 3K_S^0 K^\pm \pi^\mp$ are determined with the mixed MC samples with a certain fraction of $\chi_{cJ} \rightarrow 3K_S^0 K^\pm \pi^\mp$, $\chi_{cJ} \rightarrow 2K_S^0 K^*(892)^\pm K^\mp$, $\chi_{cJ} \rightarrow 3K_S^0 K^*(892)^0 + \text{c.c.}$ and $\chi_{cJ} \rightarrow f_X(1500)K_S^0 K^\pm \pi^\mp$. The fractions are determined from fits to the invariant mass distributions of the two-body combinations, where the signal is modeled by a signal MC shape convolved with a Gaussian function and the background by a third-order Chebyshev polynomial, and are summarized in Table II. Figures 4, 5 and 6

show the comparisons of the invariant masses of the two-body combinations of the accepted candidate events for $\chi_{c0,1,2} \rightarrow 3K_S^0 K^\pm \pi^\mp$ in data and in mixed MC samples. Here, we mark the three different K_S^0 candidates as a, b and c, and K^\pm and π^\pm as 1 and 2, respectively, to identify the different combinations. The variations of these fractions will be considered as a source of systematic uncertainty.

TABLE II. The fractions (in %) of different subprocesses in $\chi_{cJ} \rightarrow 3K_S^0 K^\pm \pi^\mp$.

	χ_{c0}	χ_{c1}	χ_{c2}
$3K_S^0 K^\pm \pi^\mp$ (PHSP)	3.1	10.0	4.7
$2K_S^0 K^*(892)^\pm K^\mp$	33.0	42.1	40.1
$3K_S^0 K^*(892)^0 + \text{c.c.}$	31.3	27.1	22.1
$f_X(1500)K_S^0 K^\pm \pi^\mp$	32.6	20.8	33.0

The products of branching fractions of $\chi_{cJ} \rightarrow 3K_S^0 K^\pm \pi^\mp$ and $\psi(3686) \rightarrow \gamma\chi_{cJ}$ are calculated as

$$\mathcal{B}_{\psi(3686) \rightarrow \gamma\chi_{cJ}} \cdot \mathcal{B}_{\chi_{cJ} \rightarrow 3K_S^0 K^\pm \pi^\mp} = \frac{N_{\chi_{cJ}}^{\text{net}}}{N_{\psi(3686)} \cdot \varepsilon \cdot \mathcal{B}(K_S^0 \rightarrow \pi^+\pi^-)}, \quad (3)$$

where $N_{\psi(3686)}$ is the total number of $\psi(3686)$ events in data, ε is the detection efficiency, and $\mathcal{B}(K_S^0 \rightarrow \pi^+\pi^-)$ is the branching fraction of $K_S^0 \rightarrow \pi^+\pi^-$ taken from the PDG [4]. The branching fractions of $\chi_{cJ} \rightarrow 3K_S^0 K^\pm \pi^\mp$ are obtained and summarized in Table III.

V. SYSTEMATIC UNCERTAINTIES

The different sources of systematic uncertainty in the branching fraction measurements are discussed below and summarized in Table IV.

The total number of $\psi(3686)$ events in data has been measured to be $N_{\psi(3686)} = (2712.4 \pm 14.3) \times 10^6$ with the inclusive hadronic data sample, as described in Ref. [8]. The uncertainty of $N_{\psi(3686)}$ is 0.5%.

The systematic uncertainties of tracking and PID efficiencies for K^\pm and π^\pm are estimated with the control samples $J/\psi \rightarrow K^*(892)\bar{K}$ and $J/\psi \rightarrow p\bar{p}\pi^+\pi^-$, respectively. They are assigned as 1.0% for each track, excluding those from K_S^0 decays [23].

The systematic uncertainty of K_S^0 reconstruction, including tracking efficiency, K_S^0 mass window, and vertex fitters quality, has been estimated by using the control samples $J/\psi \rightarrow K^*(892)^\pm \bar{K}^\mp$ and $J/\psi \rightarrow \phi K^*(892)^\pm K^\mp$. The systematic uncertainty of K_S^0 reconstruction is assigned to be 1.5% per K_S^0 [24].

The systematic uncertainty in photon detection is assigned as 1.0% per photon by studies of the control sample $J/\psi \rightarrow \pi^+\pi^-\pi^0$ [25].

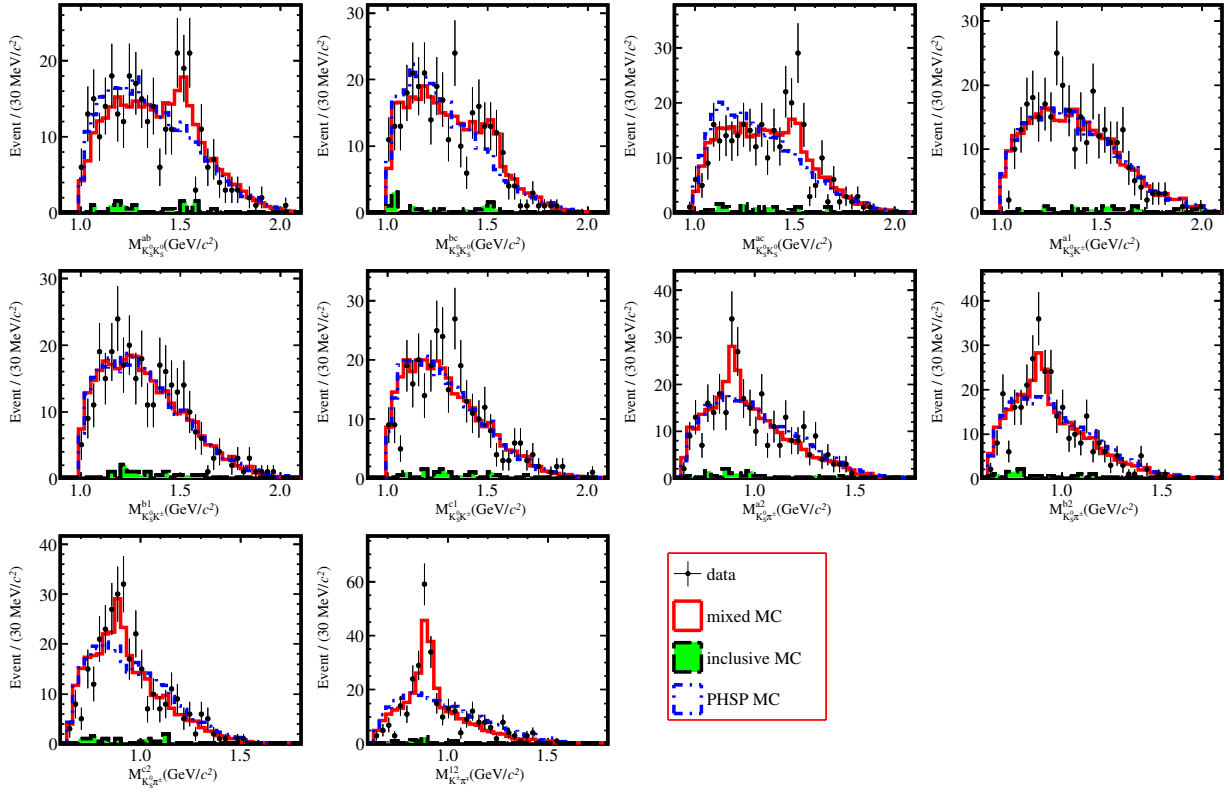


FIG. 4. Distributions of the two-body invariant masses of the accepted candidate events for $\chi_{c0} \rightarrow 3K_S^0 K^\pm \pi^\mp$. The black dots with error bars are data, the red histograms are the mixed MC sample, the cyan histograms are the PHSP signal MC sample, and the green histograms are the simulated background from the inclusive MC sample. Events have been required to be within $M_{3K_S^0 K^\pm \pi^\mp} \in [3.394, 3.434] \text{ GeV}/c^2$.

TABLE III. The quantities used to calculate the branching fractions of $\chi_{cJ} \rightarrow 3K_S^0 K^\pm \pi^\mp$, where the first uncertainties are statistical and the second systematic.

	χ_{c0}	χ_{c1}	χ_{c2}
$N_{\chi_{cJ}}^{\text{obs}}$	343 ± 22	1190 ± 37	767 ± 29
ε (%)	4.91 ± 0.07	5.18 ± 0.07	5.22 ± 0.07
$\mathcal{B}(\psi(3686) \rightarrow \gamma \chi_{cJ}) \cdot \mathcal{B}(\chi_{cJ} \rightarrow 3K_S^0 K^\pm \pi^\mp) (\times 10^{-6})$	$7.78 \pm 0.49 \pm 0.64$	$25.6 \pm 0.8 \pm 1.9$	$16.4 \pm 0.6 \pm 1.4$
$\mathcal{B}(\chi_{cJ} \rightarrow 3K_S^0 K^\pm \pi^\mp) (\times 10^{-5})$	$7.95 \pm 0.50 \pm 0.65$	$26.2 \pm 0.8 \pm 1.9$	$17.2 \pm 0.7 \pm 1.5$

To estimate the systematic uncertainties of the MC generation of the $\chi_{cJ} \rightarrow 3K_S^0 K^\pm \pi^\mp$ decays, we compare our nominal signal efficiencies with those determined from the mixed MC events after varying the relative fractions of the sub-resonant decays by $\pm 1\sigma$. The relative changes of the signal efficiencies, 0.2%, 0.1% and 0.1%, are assigned as the systematic uncertainties for χ_{c0} , χ_{c1} and χ_{c2} decays, respectively.

The systematic uncertainties of the fit to the $M_{3K_S^0 K^\pm \pi^\mp}$ distribution are considered below. The uncertainties due to the signal shape are estimated by changing the signal shape from a Breit-Wigner function convolved with a Gaussian function to the one from signal MC convolved with a Gaussian function. The uncertainties due to the fixed widths of the χ_{cJ} mesons are esti-

mated by varying the fixed world average values by $\pm 1\sigma$. The uncertainties due to the background shape are estimated by varying the nominal ones from the first-order to second-order Chebyshev polynomial functions. The uncertainties of the simultaneous fit method are estimated by changing the nominal fit to a one-dimensional fit of the $M_{3K_S^0 K^\pm \pi^\mp}$ distribution, with a background shape derived from data events in the three-dimensional K_S^0 sidebands. The uncertainties of the fit range are estimated by changing them from $[3.31, 3.61] \text{ GeV}/c^2$ to $[3.28, 3.58] \text{ GeV}/c^2$ and $[3.35, 3.65] \text{ GeV}/c^2$. Adding these uncertainties in quadrature gives the total systematic uncertainties due to the $M_{3K_S^0 K^\pm \pi^\mp}$ fit to be 5.2%, 3.3%, and 4.8% for χ_{c0} , χ_{c1} and χ_{c2} , respectively.

The systematic uncertainties from the 4C kinematic fit

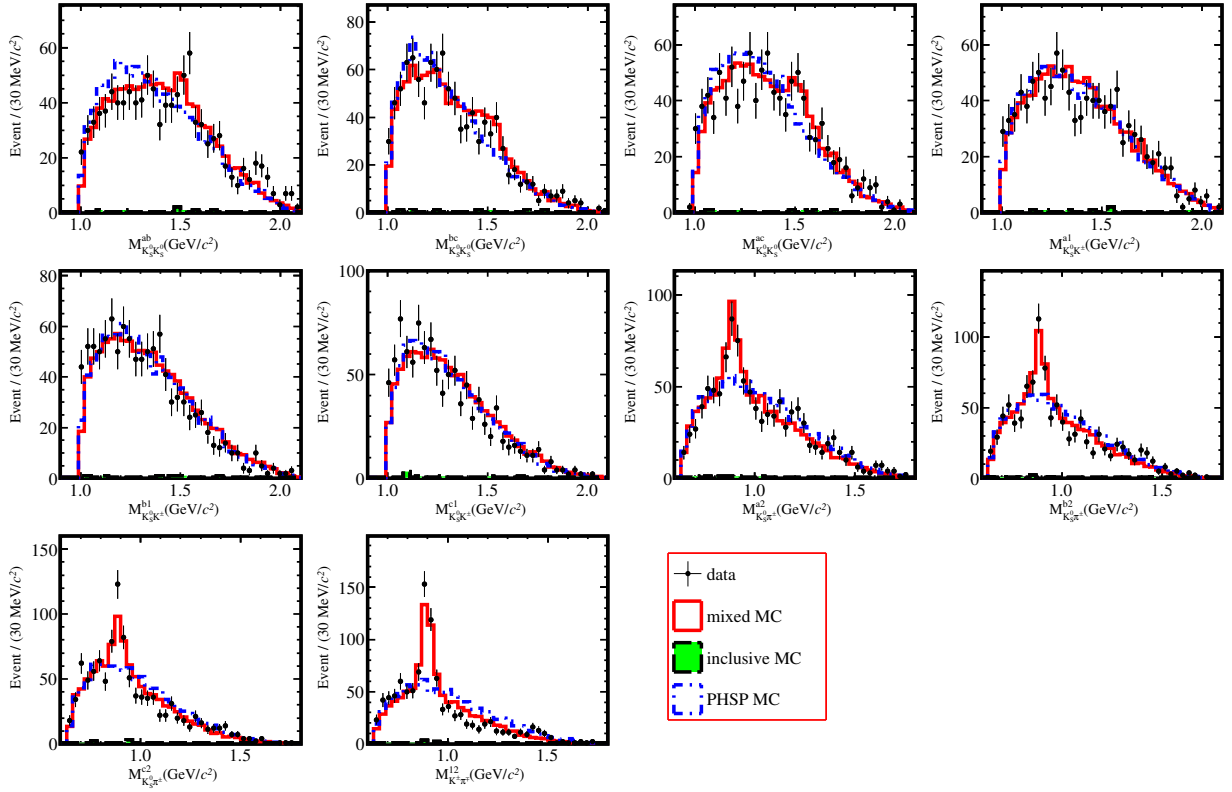


FIG. 5. Distributions of the two-body invariant masses of the accepted candidate events for $\chi_{c1} \rightarrow 3K_S^0 K^\pm \pi^\mp$. The black dots with error bars are data, the red histograms are the mixed MC sample, the cyan histograms are the PHSP signal MC sample, and the green histograms are the simulated background from the inclusive MC sample. Events have been required to be within $M_{3K_S^0 K^\pm \pi^\mp} \in [3.496, 3.526] \text{ GeV}/c^2$.

TABLE IV. Relative systematic uncertainties (in %) in the branching fraction measurements.

Source	χ_{c0}	χ_{c1}	χ_{c2}
$N_\psi(3686)$	0.5	0.5	0.5
Tracking	2.0	2.0	2.0
PID	2.0	2.0	2.0
K_S^0 reconstruction	4.5	4.5	4.5
γ selection	1.0	1.0	1.0
4C kinematic fit	1.0	1.9	1.3
$M_{3K_S^0 K^\pm \pi^\mp}$ fit	5.2	3.3	4.8
$\mathcal{B}(K_S^0 \rightarrow \pi^+ \pi^-)$	0.2	0.2	0.2
$\mathcal{B}(\psi(3686) \rightarrow \gamma \chi_{cJ})$	2.0	2.5	2.1
MC statistics	1.6	1.5	1.4
MC generation	0.2	0.1	0.1
E_γ^3 factor	1.6	1.5	3.9
Total	8.2	7.4	8.7

is estimated by comparing the signal efficiencies after and before the helix parameter correction, with parameters taken from Ref. [26]. The changes of the signal efficiencies are assigned as the systematic uncertainties, which are 1.0%, 1.9% and 1.3% for χ_{c0} , χ_{c1} and χ_{c2} .

The systematic uncertainties due to MC statistics are

1.6%, 1.5%, and 1.4% for χ_{c0} , χ_{c1} and χ_{c2} , respectively.

The uncertainties of the branching fractions quoted from the PDG [4] are 2.0%, 2.5%, and 2.1% for $\psi(3686) \rightarrow \gamma \chi_{c0,1,2}$ and 0.07% for $K_S^0 \rightarrow \pi^+ \pi^-$.

The systematic uncertainties in the E_γ^3 factor, which is used to take into account the electromagnetic transition rates of the lowest multipoles, are estimated by varying the signal shape from a Breit-Wigner function convolved with a Gaussian function to a Breit-Wigner function multiplied by the E_γ^3 factor [27]. The differences in the signal yields are assigned as the systematic uncertainties, which are 1.5%, 1.3%, and 3.9% for χ_{c0} , χ_{c1} and χ_{c2} .

For each signal decay, the total systematic uncertainty is obtained by adding all systematic uncertainties in quadrature.

VI. SUMMARY

By analyzing $(2712.4 \pm 14.3) \times 10^6$ $\psi(3686)$ events collected with the BESIII detector operating at the BEPCII collider, the decays $\chi_{c0,1,2} \rightarrow 3K_S^0 K^\pm \pi^\mp$ are observed for the first time with statistical significances greater than 10σ . Their decay branching fractions are determined to

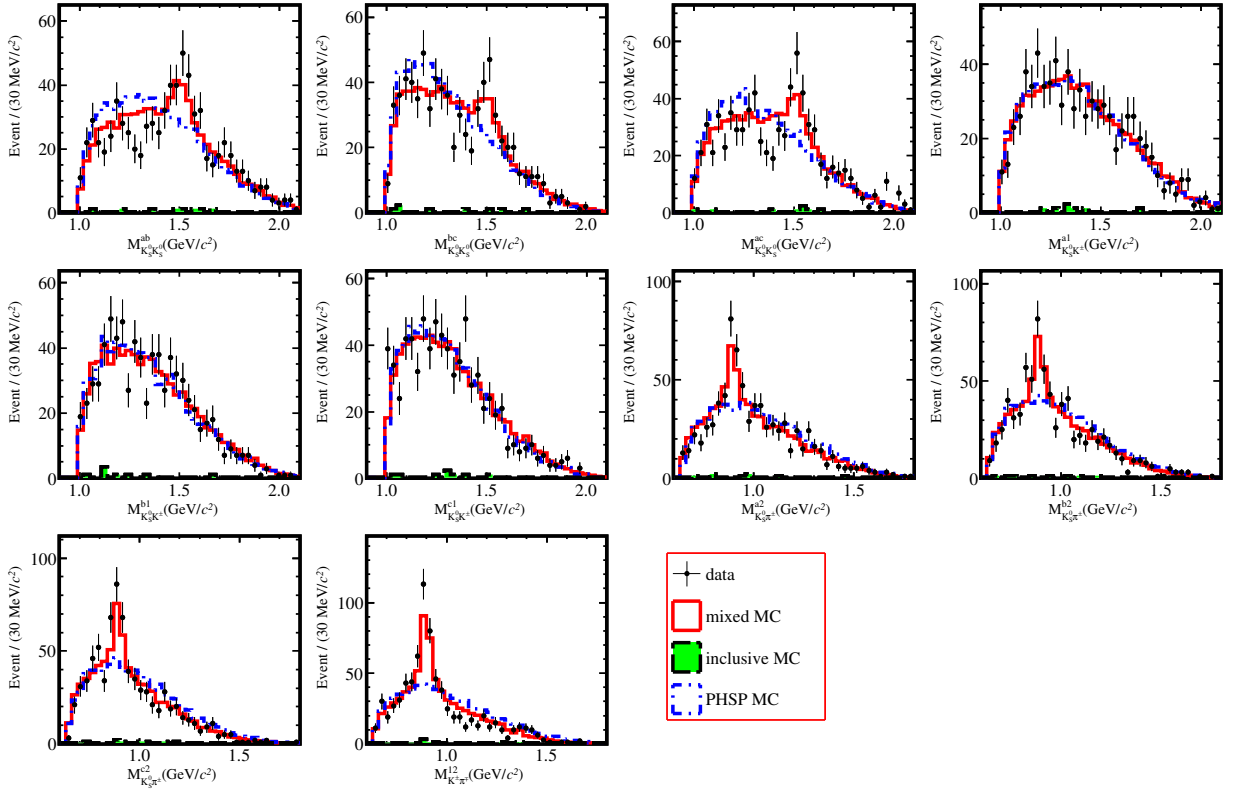


FIG. 6. Distributions of the two-body invariant masses of the accepted candidate events for $\chi_{c2} \rightarrow 3K_S^0 K^\pm \pi^\mp$. The black dots with error bars are data, the red histograms are the mixed MC sample, the cyan histograms are the PHSP signal MC sample, and the green histograms are the simulated background from the inclusive MC sample. Events have been required to be within $M_{3K_S^0 K^\pm \pi^\mp} \in [3.541, 3.571] \text{ GeV}/c^2$.

be

$$\begin{aligned}\mathcal{B}(\chi_{c0} \rightarrow 3K_S^0 K^\pm \pi^\mp) &= (7.95 \pm 0.50 \pm 0.65) \times 10^{-5}, \\ \mathcal{B}(\chi_{c1} \rightarrow 3K_S^0 K^\pm \pi^\mp) &= (2.52 \pm 0.08 \pm 0.19) \times 10^{-4}, \\ \mathcal{B}(\chi_{c2} \rightarrow 3K_S^0 K^\pm \pi^\mp) &= (1.72 \pm 0.07 \pm 0.15) \times 10^{-4}.\end{aligned}$$

After considering the intermediate states and the effects of phase space, these results are comparable with the branching fractions in Table I. Through the measurement of the branching fractions of $\chi_{cJ} \rightarrow 3K_S^0 K^\pm \pi^\mp$, it is possible to derive valuable information to deepen our understanding of the mechanisms of χ_{cJ} decays.

VII. ACKNOWLEDGMENTS

The BESIII Collaboration thanks the staff of BEPCII and the IHEP computing center for their strong support. This work is supported in part by National Key R&D Program of China under Contracts Nos. 2020YFA0406300, 2020YFA0406400, 2023YFA1606000; National Natural Science Foundation of China (NSFC) under Contracts Nos. 12035009, 11635010, 11735014,

11935015, 11935016, 11935018, 12025502, 12035013, 12061131003, 12192260, 12192261, 12192262, 12192263, 12192264, 12192265, 12221005, 12225509, 12235017, 12361141819; the Chinese Academy of Sciences (CAS) Large-Scale Scientific Facility Program; the CAS Center for Excellence in Particle Physics (CCEPP); Joint Large-Scale Scientific Facility Funds of the NSFC and CAS under Contract No. U1832207; CAS under Contract No. YSBR-101; 100 Talents Program of CAS; The Institute of Nuclear and Particle Physics (INPAC) and Shanghai Key Laboratory for Particle Physics and Cosmology; Agencia Nacional de Investigacion y Desarrollo de Chile (ANID), Chile under Contract No. ANID PIA/APOYO AFB230003; German Research Foundation DFG under Contract No. FOR5327; Istituto Nazionale di Fisica Nucleare, Italy; Knut and Alice Wallenberg Foundation under Contracts Nos. 2021.0174, 2021.0299; Ministry of Development of Turkey under Contract No. DPT2006K-120470; National Research Foundation of Korea under Contract No. NRF-2022R1A2C1092335; National Science and Technology fund of Mongolia; National Science Research and Innovation Fund (NSRF) via the Program Management Unit for Human Resources & Institutional Development, Research and Innovation of Thailand under Contracts Nos. B16F640076, B50G670107;

Polish National Science Centre under Contract No. 2019/35/O/ST2/02907; Swedish Research Council under Contract No. 2019.04595; The Swedish Foundation for International Cooperation in Research and Higher

Education under Contract No. CH2018-7756; U. S. Department of Energy under Contract No. DE-FG02-05ER41374.

-
- [1] M. Ablikim *et al.* (BESIII Collaboration), *Chin. Phys. C* **44**, 040001 (2020).
 - [2] W. Kwong, J. L. Rosner and C. Quigg, *Ann. Rev. Nucl. Part. Sci.* **37**, 325 (1987).
 - [3] E. Eichten, S. Godfrey, H. Mahlke and J. L. Rosner, *Rev. Mod. Phys.* **80**, 1161 (2008).
 - [4] S. Navas *et al.* (Particle Data Group), *Phys. Rev D* **110**, 030001 (2024).
 - [5] N. Brambilla *et al.* (Quarkonium Working Group), *CERN Yellow Reports: Monographs*, CERN-2005-005.
 - [6] H. W. Huang and K. T. Chao, *Eur. Phys. J. C* **71**, 1534 (2011).
 - [7] M. Ablikim *et al.* (BESIII Collaboration), *Phys. Rev. D* **91**, 112008 (2015).
 - [8] M. Ablikim *et al.* (BESIII Collaboration), *Chin.Phys.C* **48**, 093001(2024).
 - [9] M. Ablikim *et al.* (BESIII Collaboration), *Nucl. Instrum. Methods Phys. Res., A* **614**, 345 (2010).
 - [10] C. H. Yu *et al.*, Proceeding of IPAC2016, Busan, Korea, 2016
 - [11] X. Li *et al.*, *Radiat. Detect. Technol. Methods* **1**, 13 (2017).
 - [12] Y. X. Guo *et al.*, *Radiat. Detect. Technol. Methods* **1**, 15 (2017).
 - [13] P. Cao *et al.*, *Nucl. Instrum. Meth. A* **953**, 163053 (2020).
 - [14] S. Agostinelli *et al.* (GEANT4 Collaboration), *Nucl. Instrum. Methods Phys. Res. A* **506**, 250 (2003).
 - [15] S. Jadach, B. F. L. Ward and Z. Was, *Phys. Rev. D* **63**, 113009 (2001).
 - [16] D. J. Lange, *Nucl. Instrum. Methods Phys. Res. A* **462**, 152 (2001).
 - [17] R. G. Ping, *Chin. Phys. C* **32**, 599 (2008).
 - [18] J. C. Chen, G. S. Huang, X. R. Qi, D. H. Zhang and Y. S. Zhu, *Phys. Rev. D* **62**, 034003 (2000).
 - [19] E. Richter Was, *Phys. Lett. B* **303**, 163 (1993).
 - [20] M. Ablikim *et al.* (BESIII Collaboration), *Computer Physics Communications* **258**, 107540 (2021).
 - [21] M. Ablikim *et al.* (BESIII Collaboration), *Chin. Phys. C* **37**, 123001 (2013).
 - [22] W. M. Tanenbaum *et al.*, *Phys. Rev. D* **17**, 1731 (1978).
 - [23] M. Ablikim *et al.* (BESIII Collaboration), *Phys. Rev D* **83**, 112005(2011).
 - [24] M. Ablikim *et al.* (BESIII Collaboration). *Phys. Rev. D* **92**, 112008 (2015).
 - [25] M. Ablikim *et al.* (BESIII Collaboration). *Phys. Rev D* **83**, 112005(2011).
 - [26] M. Ablikim *et al.* (BESIII Collaboration), *Phys. Rev. D* **87**, 012002 (2013).
 - [27] V. V. Anashin, *et al.* *Int. J. Mod. Phys. Conf. Ser.* **02**, 188-192 (2011).